*Metallophysics and Advanced Technologies*
*Металофіз. новітні технол.*
*Metallofiz. Noveishie Tekhnol.*
2026, vol. 48, No. 9, pp. 949–962
https://doi.org/10.15407/mfint.48.09.0949
Reprints available directly from the publisher

© 2026 G. V. Kurdyumov Institute for Metal Physics,
National Academy of Sciences of Ukraine
Published by license under
the G. V. Kurdyumov Institute for Metal Physics–
N.A.S. of Ukraine Publishers imprint.
Printed in Ukraine.

PACS numbers: 46.25.-y, 46.50.+a, 46.70.De, 62.20.mj, 68.60.Bs, 81.40.Jj, 81.65.Mq

# On the Effect of Residual Stresses on the Strength of Oxidized Plates under Thermomechanical Loading

I. P. Shatskyi, V. M. Petrashchuk, L. Ya. Ropyak*, and O. O. Lazarieva**

*Pidstryhach Institute for Applied Problems of Mechanics and Mathematics,*
*N.A.S. of Ukraine,*
*3-b Naukova Str.,*
*UA-79060 Lviv, Ukraine*
**Ivano-Frankivsk National Technical University of Oil and Gas,*
*15 Karpatska Str.,*
*UA-76019 Ivano-Frankivsk, Ukraine*
***Zaporizhzhia Polytechnic National University,*
*64 Zhukovsky Str.,*
*UA-69063 Zaporizhzhya, Ukraine*

This paper develops a methodology for investigating the stress–strain state and evaluating the load-bearing capacity of metal plates strengthened by plasma electrolytic oxidation of the surface layer. The object of analysis is a plate of symmetric structure with a double-side oxide coating subjected to biaxial tensile loading under uniform heating and in the presence of a self-equilibrated field of residual stresses. Within the framework of the plane-sections' and elastic-deformation hypothesis, the closed-form analytical expressions are obtained for the residual stresses in the substrate and in the oxide layers in terms of the incompatible strain of the surface layers, as well as for the total stress state under combined thermomechanical loading. Two strength criteria are formulated and analysed: a global (integral) criterion, which is insensitive to self-equilibrated residual and thermal components, and a local criterion, which reduces to a set of linear inequalities for the admissible load and temperature at a given level of residual stresses. The capa-

Corresponding author: Ivan Petrovych Shatskyi
E-mail: ipshatsky@gmail.com

Citation: I. P. Shatskyi, V. M. Petrashchuk, L. Ya. Ropyak, and O. O. Lazarieva, On the Effect of Residual Stresses on the Strength of Oxidized Plates under Thermomechanical Loading, *Metallofiz. Noveishie Tekhnol.*, **48**, No. 9: 949–962 (2026). DOI: 10.15407/mfint.48.09.0949

© Publisher PH 'Akademperiodyka' of the NAS of Ukraine, 2026. This is an open access article under the CC BY-ND license (https://creativecommons.org/licenses/by-nd/4.0)

bilities of the methodology are illustrated by computational examples for the $Al/Al_2O_3$ (6061-T6 alloy/aluminium oxide) and $Ti/TiO_2$ (Grade 2 titanium/titanium dioxide) compositions, with account of the Pilling–Bedworth ratio and the mismatch of linear thermal-expansion coefficients of the metal and its oxide. As shown, in the absence of thermal effects and residual stresses, the load-bearing capacity of an oxidized plate in tension is about three times lower than that of the uncoated plate, owing to high stress concentration in the thin stiff coating. The combinations of residual-stresses' level and temperatures are identified, at which an oxidized plate operates as an equal-strength structure with maximum load-bearing capacity; explicit analytical relations are obtained for both the $Al/Al_2O_3$ and $Ti/TiO_2$ systems.

**Key words:** plasma electrolytic oxidation, oxidized plate, residual stresses, thermomechanical loading, strength.

У статті розроблено методику дослідження напружено-деформованого стану й оцінювання утримувальної здатности металевих платівок, зміцнених плазмовим електролітичним оксидуванням поверхневого шару. Об'єктом аналізи є платівка симетричної будови з двостороннім оксидним покриттям, яка зазнає двовісного розтягувального навантаження за умов рівномірного нагрівання та наявности самозрівноважного поля залишкових напружень. У рамках гіпотези стосовно пласких перерізів і пружнього деформування одержано замкнуті аналітичні залежності для залишкових напружень у підкладинці й оксидних шарах через несумісну деформацію поверхневих шарів, а також для повного напруженого стану за комбінованого термомеханічного навантаження. Сформульовано та проаналізовано два критерії міцности: глобальний (інтеґральний) критерій, нечутливий до самозрівноважних залишкових і теплових компонент, та локальний критерій, який зводиться до системи лінійних нерівностей щодо допустимого навантаження та температури за заданого рівня залишкових напружень. Можливості методики проілюстровано на прикладах композицій $Al/Al_2O_3$ (стоп 6061-T6/оксид Алюмінію) та $Ti/TiO_2$ (титан ґатунку 2/діоксид Титану) з урахуванням коефіцієнта Піллінґа–Бедворта та ріжниці коефіцієнтів лінійного теплового розширення металу та його оксиду. Показано, що за відсутности температурного впливу та залишкових напружень несна здатність оксидованої платівки за розтягу приблизно втричі менша порівняно з неоксидованою через високу концентрацію напружень у тонкому цупкому покритті. Визначено співвідношення рівнів залишкових напружень і температур, за яких оксидована платівка працює як рівноміцна конструкція з максимальною утримувальною здатністю; одержано явні аналітичні залежності для обох систем — $Al/Al_2O_3$ й $Ti/TiO_2$.

**Ключові слова:** плазмове електролітичне оксидування, оксидована платівка, залишкові напруження, термомеханічне навантаження, міцність.

*(Received 20 May, 2026; in final version, 27 May, 2026 )*

## 1. INTRODUCTION

Modern engineering design relies increasingly on the comprehensive

assessment of the strength and reliability of structural components under realistic service scenarios, as illustrated by the approaches presented in Refs. [1, 2]. The interaction between a structure and its environment, together with severe operating conditions, places stringent demands on researchers regarding corrosion protection, wear resistance, and the thermal insulation of component surfaces. Among the variety of methods available for surface strengthening of machine and mechanism parts [3–6], the method of plasma electrolytic oxidation (PEO) of valve metals occupies a special place [7–12]. Among the key advantages of PEO, there is the formation of ceramic-like layers with a developed structure, which are firmly bonded to the metallic substrate and provide a substantial enhancement of surface hardness, wear and corrosion resistance, as well as the thermal insulation characteristics of the component. At the same time, the process is environmentally safer than conventional anodizing, requires no complex preliminary surface preparation, and is readily scalable to articles of complex geometry.

However, the significant increase in the stiffness of oxidized surface layers is not always accompanied by a corresponding increase in their strength. Consequently, the transition from a ductile metal to a brittle ceramic may give rise to durability problems for coated parts. A high level of compressive residual stresses in the oxide coating frequently allows an appropriate balance between stiffness and strength to be maintained.

In general, theoretical methods for studying residual phenomena are well developed at present for plastic deformation processes [13–16] and for hysteretic energy dissipation in frictional contact [17–21]. Recent publications [22–29] cover measurement methods, the understanding of evolution, and experimental data on residual stresses in $Al/Al_2O_3$ and $Ti/TiO_2$ systems, in particular mentioning the curvature method, XRD, and the $\sin^2\psi$ method as experimental techniques. It should be noted that these publications exhibit a considerable scatter in experimental data on residual stresses in oxide coatings: from 20 to 1500 MPa, depending on the parameters of the oxidation process and the measurement techniques.

Analytical models of thermal stresses providing closed-form solutions for the stress distribution in layered structures under thermomechanical loading are described in Refs. [30–36]. The influence of nonstationary temperature variations is taken into account in Refs. [37–39]. Singular problems concerning the behaviour of layered and functionally graded coatings under localized contact loading have been the subject of investigations [40–44].

Issues of fracture mechanics and damage propagation criteria for structures with coatings are usually treated without accounting for residual phenomena [45–51]. An exception is paper [52], which de-

scribes models for the failure modes of PEO coatings under the influence of tensile and compressive residual stresses. Problems concerning the limit equilibrium of cracked thin-walled structures under combined loading were considered in Refs. [53–55].

The literature review presented above motivates the investigation of the strength of oxidized plates of symmetric structure under two-parameter loading over a wide range of variation of residual stresses.

The aim of the present paper is to develop an engineering methodology for the analytical estimation of the influence of residual stresses on the strength of double-side oxidized plates subjected to thermomechanical loading.

## 2. MATERIALS AND METHODS

### 2.1. Geometry of the Oxidized Plate

Consider a metal plate of initial thickness $h_s^0$. After oxidation of its surfaces, a symmetric composite structure is formed, consisting of a substrate of thickness $h_s$ and two surface layers (films) of thickness $h_f$ (Fig. 1). Hereinafter, all quantities pertaining to the substrate and the coating will be denoted by the indices 's' and 'f', respectively.

The following relations hold: $h_s = h_s^0 - 2(1-\alpha)h_f$, $h_s + 2h_f = h_s^0 + \alpha h_f$, where $\alpha = R_{PB} - 1$, and $R_{PB}$ is the Pilling–Bedworth ratio [56, 57].

Let $z$ be the transverse coordinate measured from the midsurface of the plate. Then, $H_s = \{z: |z| < h_s/2\}$ is the region occupied by the substrate, $H_f = \{z: h_s/2 < |z| < h_s/2 + h_f\}$ is the coating zone, $H = H_s + H_f = \{z: 0 \le |z| \le h_s/2 + h_f\}$ is the full cross-section.

### 2.2. Determination of Residual Stresses

We represent the total in-plane strain of the plate, which is nonhomogeneous through the thickness, as a superposition of the elastic strain $(1-\nu)\sigma/E$ and the generally incompatible strain $\varepsilon^0$ induced by fields of

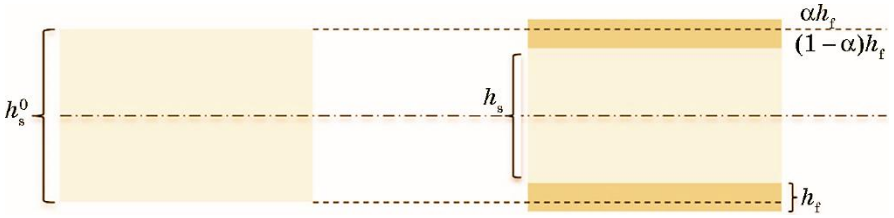



**Fig. 1.** Sketch of the cross-section of an oxidized plate.

nonmechanical nature: $\varepsilon = \dfrac{1-\nu}{E}\sigma + \varepsilon^0$.

For the stresses, we then obtain the expression

$$\sigma(z) = \frac{E(z)}{1-\nu(z)}(\varepsilon - \varepsilon^0(z)); \tag{1}$$

$E(z) = \begin{cases} E_f, z \in H_f, \\ E_s, z \in H_s \end{cases}$ is the Young's modulus and $\nu(z) = \begin{cases} \nu_f, z \in H_f, \\ \nu_s, z \in H_s \end{cases}$ is the Poisson's ratio of the material.

We require that the stresses have the status of residual stresses ($\sigma = \sigma_{res}$), that is, they must be self-equilibrated.

Then, taking into account formula (1) and the plane-sections' hypothesis, we obtain:

$$\varepsilon_{res}\int_H \frac{E(z)}{1-\nu(z)}dz - \int_H \frac{E(z)}{1-\nu(z)}\varepsilon^0(z)dz = 0, \tag{2}$$

and the residual stresses are expressed in terms of the incompatible strain:

$$\sigma_{res}(z) = \frac{E(z)}{1-\nu(z)}\left(\frac{\displaystyle\int_H \frac{E(z)}{1-\nu(z)}\varepsilon^0(z)dz}{\displaystyle\int_H \frac{E(z)}{1-\nu(z)}dz} - \varepsilon^0(z)\right). \tag{3}$$

In the case of oxidation of both surfaces, we have an even function

$$\varepsilon^0(z) = \begin{cases} \varepsilon_f^0, z \in H_f, \\ 0, z \in H_s. \end{cases} \tag{4}$$

By evaluating the integrals in formula (2), we find expressions for the residual stresses in terms of the incompatible strain of the oxidized surface layers:

$$\sigma_{res,f} = -\frac{\dfrac{E_s h_s}{1-\nu_s}}{\dfrac{E_s h_s}{1-\nu_s} + \dfrac{2E_f h_f}{1-\nu_f}}\frac{E_f}{1-\nu_f}\varepsilon_f^0, \quad \sigma_{res,s} = \frac{\dfrac{2E_f h_f}{1-\nu_f}}{\dfrac{E_s h_s}{1-\nu_s} + \dfrac{2E_f h_f}{1-\nu_f}}\frac{E_s}{1-\nu_s}\varepsilon_f^0. \tag{5}$$

Of course, these stresses are self-equilibrated:

$$\sigma_{res,s}h_s + 2\sigma_{res,f}h_f = 0. \tag{6}$$

In addition, the residual stresses in the plate may also be expressed

in terms of the residual strain. Specifically, using relations (2)–(4) and (6), we find:

$$\sigma_{\text{res, f}} = -\frac{E_{\text{s}}}{1-\nu_{\text{s}}}\frac{h_{\text{s}}}{2h_{\text{f}}}\varepsilon_{\text{res}},\ \sigma_{\text{res, s}} = \frac{E_{\text{s}}}{1-\nu_{\text{s}}}\varepsilon_{\text{res}}. \tag{7}$$

These formulas serve to determine the residual stresses from the experimentally measured $\varepsilon_{\text{res}}$.

### 2.3. Stress State under Thermomechanical Loading

Let an oxidized plate undergo biaxial tension by uniformly distributed line forces $N = \text{const}$, be heated to a constant temperature, $\Delta T = \text{const}$, and be in the field of residual stresses (5) (the same as Eq. (7)).

We determine the stress distribution in this piecewise-homogeneous plate. Integrating expression (1) and recalling the plane-sections' hypothesis, we obtain: $N = \varepsilon\int\limits_H \frac{E(z)}{1-\nu(z)}dz - \int\limits_H \frac{E(z)}{1-\nu(z)}\varepsilon^0(z)dz$. Hence,

$\varepsilon = \dfrac{N + \int\limits_H \frac{E(z)}{1-\nu(z)}\varepsilon^0(z)dz}{\int\limits_H \frac{E(z)}{1-\nu(z)})dz}$, and finally,

$$\sigma(z) = \frac{E(z)}{1-\nu(z)}\left(\frac{N + \int\limits_H \frac{E(z)}{1-\nu(z)}\varepsilon^0(z)dz}{\int\limits_H \frac{E(z)}{1-\nu(z)}dz} - \varepsilon^0(z)\right). \tag{8}$$

We take into account that now $\varepsilon^0(z) = \begin{cases}\varepsilon_{\text{f}}^0 + \alpha_{\text{f}}\Delta T,\ z \in H_{\text{f}},\\ \alpha_{\text{s}}\Delta T,\ z \in H_{\text{s}},\end{cases}$ where $\alpha_{\text{s}}$, $\alpha_{\text{f}}$ are the coefficients of linear thermal expansion of the metal and its oxide. After evaluating all the integrals in formula (8), we find the stresses in the coatings and in the substrate:

$$\begin{aligned}\sigma_{\text{f}} &= \frac{E_{\text{f}}/(1-\nu_f)}{E_{\text{s}}h_{\text{s}}/(1-\nu_{\text{s}}) + 2E_{\text{f}}h_{\text{f}}/(1-\nu_{\text{f}})}\left(N + \frac{E_{\text{s}}h_{\text{s}}}{1-\nu_{\text{s}}}(\alpha_{\text{s}} - \alpha_{\text{f}})\Delta T\right) + \sigma_{\text{res, f}},\\ \sigma_{\text{s}} &= \frac{E_{\text{s}}/(1-\nu_{\text{s}})}{E_{\text{s}}h_{\text{s}}/(1-\nu_{\text{s}}) + 2E_{\text{f}}h_f/(1-\nu_{\text{f}})}\left(N - \frac{2E_{\text{f}}h_{\text{f}}}{1-\nu_{\text{f}}}(\alpha_{\text{s}} - \alpha_{\text{f}})\Delta T\right) + \sigma_{\text{res, s}}.\end{aligned} \tag{9}$$

This result demonstrates the influence of the mechanical load, heating, and residual stresses on the stress state of an oxidized plate of

symmetric structure.

### 2.4. Effect of Residual Stresses on Strength

We begin with an analysis for the uncoated plate ($h_f = 0$, $h_s = h_s^0$). In this case,

$$\sigma_s = N / h_s^0, \tag{10}$$

while thermal and residual stresses are absent.

From the strength condition

$$\sigma_s \le [\sigma]_s,$$

we find the allowable load for the unoxidized plate:

$$N \le N_c^0 = [\sigma]_s h_s^0. \tag{11}$$

This is the baseline result, with which all subsequent results will be compared.

We write the strength conditions for the inhomogeneous plate in terms of the allowable stresses for its components:

$$\sigma(z) \le [\sigma](z) = \begin{cases} [\sigma]_f, & z \in H_f, \\ [\sigma]_s, & z \in H_s. \end{cases} \tag{12}$$

Integrating inequality (12) through the thickness, we obtain the integral (global) limit equilibrium criterion:

$$N \le N_c^{\text{global}} = [\sigma]_s h_s + 2[\sigma]_f h_f, \tag{13}$$

which is independent of the self-equilibrated thermal components and residual phenomena.

We now consider the local situation.

The strength condition (12) requires the simultaneous fulfilment of the inequalities:

$$\begin{cases} \sigma_f \le [\sigma]_f, \\ \sigma_s \le [\sigma]_s. \end{cases} \tag{14}$$

Since the stresses $\sigma_s$, $\sigma_f$ depend linearly on $N$, $\Delta T$ and on the residual stresses, set (14) is nothing other than a set of linear inequalities for the allowable loads and temperatures at a given level of residual stresses. Indeed, on the basis of result (9), conditions (14) can be rewritten in nondimensional form as follow:

$$\begin{cases} \dfrac{E_f/(1-\nu_f)}{E_s h_s/(1-\nu_s)+2E_f h_f/(1-\nu_f)}\,\dfrac{(N+E_s h_s(\alpha_s-\alpha_f)\Delta T/(1-\nu_s))}{[\sigma]_f-\sigma_{res,f}} \le 1, \\ \dfrac{E_s/(1-\nu_s)}{E_s h_s/(1-\nu_s)+2E_f h_f/(1-\nu_f)}\,\dfrac{(N-2E_f h_f(\alpha_s-\alpha_f)\Delta T/(1-\nu_f))}{[\sigma]_s-\sigma_{res,s}} \le 1. \end{cases} \tag{15}$$

For prescribed residual stresses, set (15) defines a region of safe thermomechanical loading on the plane $(N, \Delta T)$. In the general case, the simplex method must be employed to construct the solution of these inequalities. In analytical form, this is a cumbersome procedure. Therefore, we shall proceed differently. Taking into account that $\sigma_{res,\,s} = -2\sigma_{res,\,f} h_f/h_s$ (see Eq. (6)), we shall assume that $N = N(\Delta T, \sigma_{res,\,f})$. Then, from inequalities (15), we obtain the allowable load according to the local criterion in the form

$$N \le N_c^{local} = \min\left\{ \frac{-E_s h_s(\alpha_s-\alpha_f)\Delta T}{1-\nu_s} + \frac{\dfrac{E_s h_s}{1-\nu_s}+\dfrac{2E_f h_f}{1-\nu_f}}{\dfrac{E_f}{1-\nu_f}}([\sigma]_f-\sigma_{res,f}), \right.$$
$$\left. \frac{2E_f h_f}{1-\nu_f}(\alpha_s-\alpha_f)\Delta T + \frac{\dfrac{E_s h_s}{1-\nu_s}+\dfrac{2E_f h_f}{1-\nu_f}}{\dfrac{E_s}{1-\nu_s}}\left([\sigma]_s+\frac{2h_f}{h_s}\sigma_{res,f}\right) \right\}. \tag{16}$$

## 3. RESULTS AND DISCUSSION

### 3.1. Computational Examples

Detailed calculations using formulas (11), (13), and (16) were performed

**TABLE 1.** Physical and mechanical properties of the materials.

| | Aluminium (6061-T6) | Aluminium oxide $Al_2O_3$ | Titanium (Grade 2) | Titanium oxide $TiO_2$ |
|---|---|---|---|---|
| $h_s$, $h_f$, mm | 6 | 0.3 | 6 | 0.03 |
| RPB | – | 1.28 | – | 1.73 |
| $E_s$, $E_f$, GPa | 68.9 | 370 | 103 | 230 |
| $\nu_s$, $\nu_f$ | 0.33 | 0.22 | 0.34 | 0.27 |
| $\alpha_s$, $\alpha_f$, $10^{-6}$, $deg^{-1}$ | 23.6 | 8.1 | 8.6 | 8.8 |
| $[\sigma]_s$, $[\sigma]_f$, MPa | 276 | 350 | 275 | 140 |

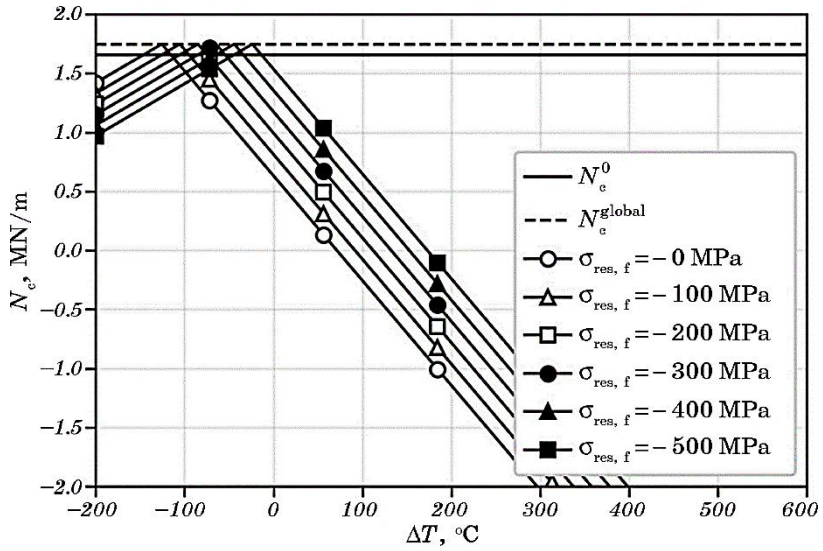



**Fig. 2.** Dependence of the allowable load on temperature at fixed levels of residual stress in the oxidized aluminium plate.

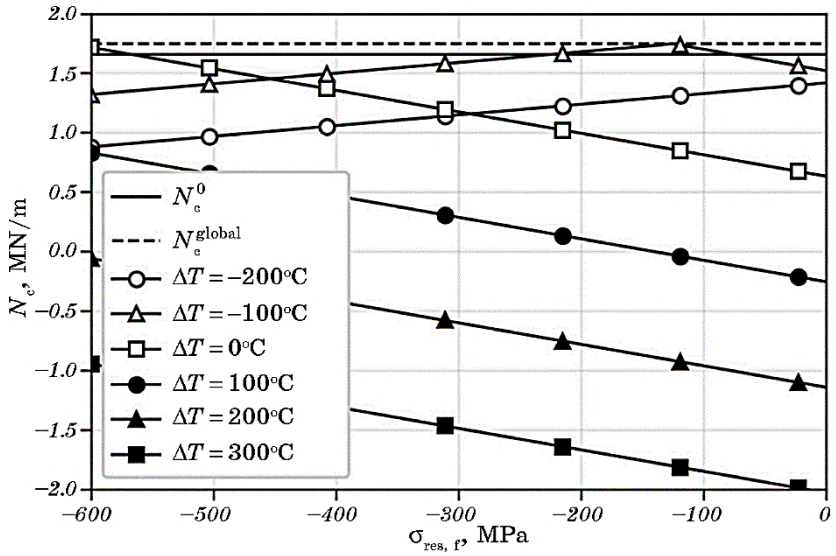



**Fig. 3.** Dependence of the allowable load on residual stress at fixed values of temperature in the oxidized aluminium plate.

for two materials, whose characteristics are listed in Table 1 [7, 58].

In Figs. 2, 3 and in Figs. 4, 5, the results of the computations of allowable loads for the oxidized aluminium-alloy plate and those for the

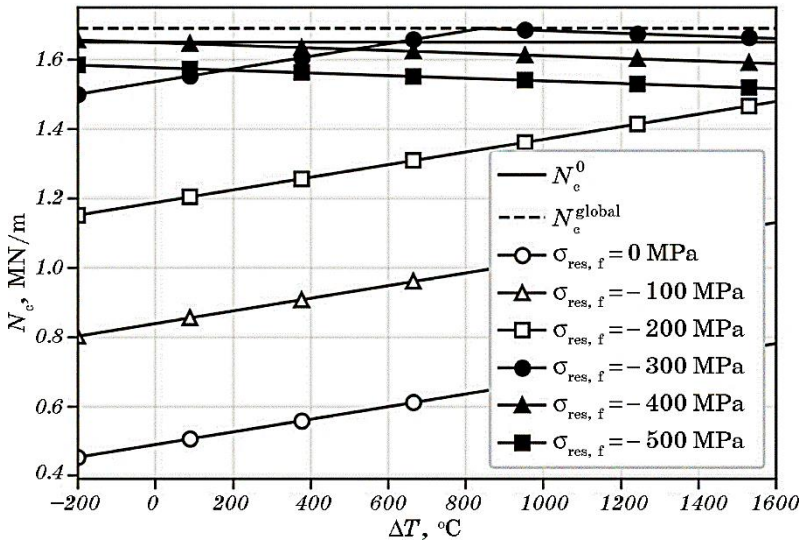



**Fig. 4.** Dependence of the allowable load on temperature at fixed levels of residual stress in the oxidized titanium plate.

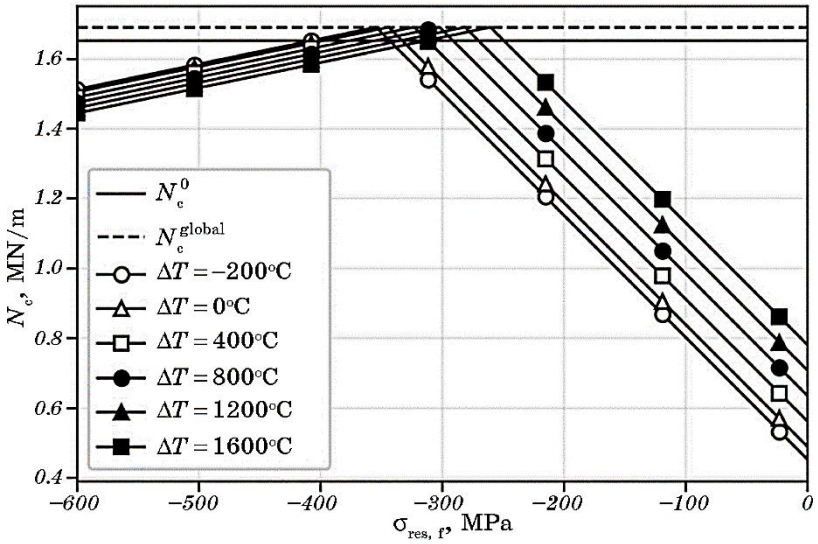



**Fig. 5.** Dependence of the allowable load on residual stress at fixed values of temperature in the oxidized titanium plate.

oxidized titanium plate are shown, respectively. All plots are compared with the horizontal line $N_c = N_c^0$ representing the allowable load for the uncoated plates.

### 3.2. Analysis of the Results

As is evident from the results presented, in the absence of thermal effects and residual stresses, the load-bearing capacity of the oxidized plates in tension is approximately three times lower than that of the uncoated plates: $N_c^{local} \approx N_c^0 / 3$. This occurs because of the high stress concentration in the thin, stiff coatings, which, owing to their limited strength, fail first.

In the presence of an additional temperature field and residual phenomena, the oxidized aluminium and titanium plates behave under loading in different ways.

Because the thermal expansion of the aluminium alloy is significantly greater than that of corundum, when the oxidized plate is heated, the coating cracks even in the absence of mechanical loading. In this case, an increase in the magnitude of the compressive residual stresses raises the allowable load at $\Delta T > -50$°C (Fig. 2). In the cryogenic temperature range, excessive compressive residual stresses in the coating are undesirable (Figs. 2 and 3), since, together with the mechanical load, they may cause additional tension and failure of the substrate.

The maximum allowable load is $N_c^{local} \approx N_c^{global}$ observed at a sub-zero temperature linked to the residual stress by the relation:

$$\Delta T = -\frac{1}{\alpha_s - \alpha_f}\left(\frac{[\sigma]_s + 2h_f\sigma_{res,f} / h_s}{E_s / (1-\nu_s)} - \frac{[\sigma]_f - \sigma_{res,f}}{E_f / (1-\nu_f)}\right).$$

In this case, the oxidized aluminium plate operates as an equal-strength structure.

By contrast, in the Ti–$TiO_2$ composition, the thermal strains of the coating and the substrate are practically compatible; therefore, the system responds well to high-temperature heating and, in the presence of substantial compressive residual stresses, can sustain external tensile loads not significantly lower than those tolerated by the unoxidized titanium plate (Figs. 4 and 5). The highest load-bearing capacity according to the local criterion is achieved at an optimal level of residual stress that depends on temperature:

$$\sigma_{res,f} = -\frac{\dfrac{1-\nu_s}{E_s}[\sigma]_s - \dfrac{1-\nu_f}{E_f}[\sigma]_f + (\alpha_s - \alpha_f)\Delta T}{\dfrac{1-\nu_s}{E_s}\dfrac{2h_f}{E_s h_s} + \dfrac{1-\nu_f}{E_f}}.$$

Finally, it should be noted that the proposed analysis does not aim to describe the mechanisms of delamination of composite structures along the interface.

## 4. CONCLUSION

Thus, a methodology has been developed for investigating the stress–strain state of metal plates strengthened by plasma electrolytic oxidation of the surface layer. The methodology makes it possible to construct analytical estimates of the load-bearing capacity of oxidized plates under tensile loading, accounting for the influence of the temperature field and self-equilibrated residual stresses. The capabilities of the methodology have been illustrated by computational examples for aluminium- and titanium-based compositions. Levels of residual stresses and temperatures have been identified, at which an oxidized plate operates as an equal-strength structure, providing the highest load-bearing capacity.

This contribution was created under the support of the National Research Foundation of Ukraine (project number NRFU 2023.04/0160, 0124U003748 'Development of technology for the formation of heat-resistant coatings by plasma electrolytic oxidation on parts of aviation and rocket and space technics').

## AUTHORS' CONTRIBUTIONS

I.P.S. devised the principal conceptual framework, supervised the project, and verified the analytical approach. V.M.P. performed the analytical derivations, prepared the numerical computations, and drafted the manuscript with input from all authors. L.Ya.R. contributed to the methodology of evaluating residual stresses in oxide coatings produced by plasma electrolytic oxidation and reviewed the engineering applications. O.O.L. carried out the parametric calculations for the aluminium- and titanium-based compositions, prepared the figures, and assisted with the literature review. All authors discussed the results and approved the final version of the manuscript.

## REFERENCES

1. O. Kozak, A. Velychkovych, and A. Andrusyak, *Eng.*, **6**, Iss. 10: 269 (2025).
2. E. I. Kryzhanivs'kyi, V. P. Rudko, and I. P. Shats'kyi, *Mater. Sci.*, **40**: 547 (2004).
3. L. Jeremić, B. Đorđević, S. Sedmak, A. Sedmak, M. Rakin, and M. Aranđelović, *Struct. Integr. Life*, **18**, No. 2: 99 (2018).
4. V. V. Kukhar, E. S. Klimov, and S. M. Chernenko, *Solid State Phenomena*, **316**: 873 (2021).
5. V. B. Tarelnyk, O. P. Gaponova, O. M. Myslyvchenko, and B. O. Sarzhanov, *Powder Metall. Met. Ceram.*, **59**: 76 (2020).
6. P. Prysyazhnyuk, M. Bembenek, I. Drach, A. Korzhov, L. Romanyshyn, and L. Ropyak, *Management Systems Production Eng.*, **32**, Iss. 2: 294 (2024).

7. A. L. Yerokhin, X. Nie, A. Leyland, A. Matthews, and S. J. Dowey, *Surf. Coat. Technol.*, **122**, Iss. 2–3: 73 (1999).
8. M. M. Student, I. B. Ivasenko, V. M. Posuvailo, H. H. Veselivs'ka, A. Y. Pokhmurs'kyi, Y. Y. Sirak, and V. M. Yus'kiv, *Mater. Sci.*, **54**: 899 (2019).
9. F. Simchen, M. Sieber, A. Kopp, and T. Lampke, *Coatings*, **10**, Iss. 7: 628 (2020).
10. L. Ropyak, T. Shihab, A. Velychkovych, V. Bilinskyi, V. Malinin, and M. Romaniv, *Ceramics*, **6**, Iss. 1: 146 (2023).
11. L. Ropyak, T. Shihab, A. Velychkovych, O. Dubei, T. Tutko, and V. Bilinskyi, *Progress in Physics of Metals*, **24**, No. 2: 319 (2023).
12. V. Korzhyk, V. Kopei, P. Stukhliak, O. Berdnikova, O. Kushnarova, O. Kolisnichenko, O. Totosko, D. Stukhliak, and L. Ropyak, *Materials*, **18**, Iss. 15: 3620 (2025).
13. M. M. Kundrat, *Int. Applied Mechanics*, **33**: 394 (1997).
14. Y. Y. Hu and W. M. Huang, *J. Appl. Phys.*, **96**: 4154 (2004).
15. O. S. Anishchenko, V. V. Kukhar, A. V. Grushko, I. V. Vishtak, A. H. Prysiazhnyi, and E. Y. Balalayeva, *Mater. Sci. Forum*, **945**: 531 (2019).
16. V. B. Kopei, O. R. Onysko, V. G. Panchuk, Z. M. Odosii, and Y. M. Kusyi, *J. Phys.: Conf. Ser.*, **2540**: 012033 (2023).
17. A. A. Bedzir, I. P. Shatskii, and V. M. Shopa, *Int. Applied Mechanics*, **31**: 351 (1995).
18. I. P. Shats'kyi, O. M. Lyskanych, and V. A. Kornuta, *Strength Mater.*, **48**: 469 (2016).
19. I. Shatskyi, I. Popadyuk, and A. Velychkovych, *Dynamical Systems in Applications* (Ed. J. Awrejcewicz) (Łódź–Cham: Springer: 2018), p. 343.
20. I. Shatskyi and V. Perepichka, *Dynamical Systems in Applications* (Ed. J. Awrejcewicz) (Łódź–Cham: Springer: 2018), p. 335.
21. R. V. Bondarenko, I. P. Shatskyi, Ya. V. Doroshenko, and A. S. Velychkovych, *J. Achiev. Mater. Manuf. Eng.*, **132**, Nos. 1–2: 13 (2025).
22. J. Dean, T. Gu, and T. W. Clyne, *Surf. Coat. Technol.*, **269**: 47 (2015).
23. D. Shen, J. Cai, C. Guo, G. Li, D. He, and Q. Yang, *Chin. J. Mech. Eng.*, **26**: 1149 (2013).
24. R. H. U. Khan, A. L. Yerokhin, T. Pilkington, A. Leyland, and A. Matthews, *Surf. Coat. Technol.*, **200**, Iss. 5–6: 1580 (2005).
25. M. Aliofkhazraei, D. D. Macdonald, E. Matykina, E. V. Parfenov, V. S. Egorkin, J. A. Curran, S. C. Troughton, S. L. Sinebryukhov, S. V. Gnedenkov, T. Lampke, F. Simchen, and H. F. Nabavi, *Appl. Surf. Sci. Adv.*, **5**: 100121 (2021).
26. J. A. Curran and T. W. Clyne, *Surf. Coat. Technol.*, **199**, Iss. 2–3: 168 (2005).
27. D. Wojtas, M. Marciszko-Wiąckowska, and Ł. Maj, *Prog. Surf. Sci.*, **100**, Iss. 3: 100780 (2025).
28. J. Zhang, W. Dai, X. Wang, Y. Wang, H. Yue, Q. Li, X. Yang, and C. Guo, *J. Mater. Res. Technol.*, **25**: 4554 (2023).
29. A. Maytorena-Sánchez, J. Hernández-Torres, F. López-Huerta, M. A. Hernández-Campos, L. Zamora-Peredo, M. Pacio-Castillo, L. E. Serrano-De la Rosa, and L. García-González, *Mater. Lett.*, **282**: 128679 (2021).
30. C. H. Hsueh, *Thin Solid Films*, **418**, Iss. 2: 182 (2002).
31. C. H. Hsueh, *J. Appl. Phys.*, **91**, Iss. 12: 9652 (2002).

32. C. H. Hsueh and A. G. Evans, *J. Am. Ceram. Soc.*, **68**, Iss. 5: 241 (1985).
33. G. C. A. M. Janssen, M. M. Abdalla, F. van Keulen, B. R. Pul, and J. G. C. de Ree, *Thin Solid Films*, **517**, Iss. 6: 1858 (2009).
34. L. B. Freund and S. Suresh, *Thin Film Materials: Stress, Defect Formation and Surface Evolution* (Cambridge: Cambridge University Press: 2003).
35. Y. C. Tsui and T. W. Clyne, *Thin Solid Films*, **306**, Iss. 1: 23 (1997).
36. N. Dolgov, L. Vinogradov, I. Blumbergs, and R. Chatys, *Fatigue and Fracture of Materials and Structures* (Eds. G. Lesiuk, S. Duda, J. A. F. O. Correia, and A. M. P. De Jesus) (Cham: Springer: 2022), p. 9.
37. R. Kulchytsky-Zhyhailo, S. J. Matysiak, and A. S. Bajkowski, *J. Therm. Stresses*, **41**, Iss. 9: 1169 (2018).
38. V. A. Shevchuk, *J. Math. Sci.*, **278**: 780 (2024).
39. B. M. Kalynyak and V. A. Shevchuk, *Mater. Sci.*, **61**: 110 (2025).
40. S. A. G. Oliveira and A. F. Bower, *Wear*, **198**, Iss. 1–2: 15 (1996).
41. I. Shatskyi, M. Makoviichuk, L. Ropyak, and A. Velychkovych, *Ceramics*, **6**, Iss. 3: 1879 (2023).
42. I. Shatskyi, M. Makoviichuk, and L. Ropyak, *Proc. Struct. Integr.*, **59**: 407 (2024).
43. L. Ropyak, I. Shatskyi, M. Makoviichuk, and I. Lazariev, *Proc. Struct. Integr.*, **72**: 20 (2025).
44. I. Shatskyi, M. Makoviichuk, I. Lazariev, and L. Ropyak, *Struct. Integr. Life*, **25**, No. 3: 399 (2025).
45. J. W. Hutchinson and Z. Suo, *Adv. Appl. Mech.*, **29**: 63 (1992).
46. Z. C. Xia and J. W. Hutchinson, *J. Mech. Phys. Solids*, **48**, Iss. 6–7: 1107 (2000).
47. H. H. Yu and J. W. Hutchinson, *Int. J. Fracture*, **113**: 39 (2002).
48. A. G. Evans, D. R. Mumm, J. W. Hutchinson, G. H. Meier, and F. S. Pettit, *Prog. Mater. Sci.*, **46**, Iss. 5: 505 (2001).
49. I. P. Shatskyi, M. V. Makoviichuk, and A. B. Shcherbii, *Mater. Sci.*, **55**: 484 (2020).
50. I. Shatskyi and V. Petrashchuk, *Proc. Struct. Integr.*, **81**: 129 (2026).
51. I. Shatskyi, M. Makoviichuk, R. Bondarenko, and Ya. Doroshenko, *Proc. Struct. Integr.*, **81**: 240 (2026).
52. M. D. Thouless, *J. Vac. Sci. Technol. A*, **9**, Iss. 4: 2510 (1991).
53. I. P. Shatskii, *Sov. Mater. Sci.*, **25**: 160 (1989).
54. I. P. Shats'kyi and V. V. Perepichka, *Mater. Sci.*, **40**: 240 (2004).
55. I. P. Shats'kyi and M. V. Makoviichuk, *Mater. Sci.*, **41**: 486 (2005).
56. N. B. Pilling and R. E. Bedworth, *J. Inst. Met.*, **29**: 529 (1923).
57. C. Xu and W. Gao, *Mater. Res. Innov.*, **3**: 231 (2000).
58. M. Shokouhfar, C. Dehghanian, and A. Baradaran, *Appl. Surf. Sci.*, **257**, Iss. 7: 2617 (2011).